Available online at www.sciencedirect.com
SCIENCE DIRECT®
Polymer 44 (2003) 6959–6964
polymer
www.elsevier.com/locate/polymer

Effects of injection moulding induced morphology on the fracture behaviour of virgin and recycled polypropylene

J. Aurrekoetxea[a,*], M.A. Sarrionandia[a], I. Urrutibeascoa[a], M.Ll. Maspoch[b]

[a]*Department of Mechanics, Faculty of Engineering, Mondragon Unibertsitatea, 20500 Mondragon, Spain*
[b]*Dept. Ciència dels Materials i Eng. Met. Centre Català del Plàstic, Universitat Politècnica de Catalunya, C/Colom 114, 08222 Terrassa, Barcelona, Spain*

Received 13 January 2003; received in revised form 18 May 2003; accepted 3 June 2003

Abstract

The effect of injection moulding induced morphology on the fracture behaviour of virgin and recycled polypropylene (PP) has been studied. Skin-core morphology has been analysed by microhardness measurements, since the microhardness and the degree of crystallinity are directly related. Virgin PP has shown higher microhardness values and bigger plastically deformed zone at the crack tip than recycled one. These two differences are due to the higher crystallinity of the recycled PP.

Otherwise, in both materials, skin layer has shown lower microhardness values and smaller plastic zone extension than the core region. The former phenomenon is suggested to be governed by the different degrees of crystallinity between both regions, whereas the latter is related to the stress-state (triaxial stress-state) rather than to morphological parameters.

Keywords: Polypropylene; Recycling; Fracture

1. Introduction

Recycling of plastic materials is strategically very important for the environmental policy of industry. This is especially true for high consumption plastics as polypropylene (PP). The key factor to the success of PP is its versatility, which is due to the fact that the structure and properties of PP can be tailored to requirements.

Fracture toughness, as a material parameter that implies stiffness, strength and strain to failure, is of basic importance for application fields in which recycled plastics are subjected to impact and severe safety requirements have to be fulfilled by the designer. It has been shown [1,2] that the six times recycled polypropylene has worse fracture properties (K_{Ic} and G_{Ic}) than virgin one. Macroscopic morphology and mechanical properties have justified fracture behaviour differences, but all these parameters are average values and there are strong evidences that the injection moulded specimens have a gradient of morphology and properties. Fracture surface analysis has also shown that the fracture micromechanisms are not the same along the fracture surface.

In fact, fracture properties and failure micromechanisms of plastics are strongly influenced by two principal areas: first, the external conditions, e.g. temperature, strain rate, presence of geometrical discontinuities as cracks, type of loading and environment. Secondly, these properties are influenced by the microstructural parameters, which include crystalline structure, degree of crystallinity, supermolecular structure or skin-core configuration.

It is sometimes found in practice that the measured K_{Ic}, or G_{Ic}, for some materials varies with the specimen thickness, over a particular range [3]. Under full plane-strain conditions plastic deformation is constraint and represents the lower bound to the material toughness. As the constraint decreases plastic deformation will increase and fracture toughness may be expected to increase, reaching an upper limit for pure plane-stress conditions. This phenomenon is of considerable importance in edge notch specimens, where the central region gives rise to plane-strain conditions while the surfaces are in plane-stress. This will result in a distribution of fracture toughness across the section, and any measured value is an average.

Williams and Parvin [4,5] have assumed that a useful

* Corresponding author. Tel.: +34-943-79-14-36; fax: +34-943-79-47-00.
E-mail address: jaurrekoetxea@eps.mondragon.edu (J. Aurrekoetxea).

0032-3861/03/$ - see front matter © 2003 Published by Elsevier Ltd.
doi:10.1016/S0032-3861(03)00493-2

approximation to the distribution is obtained by assuming a bimodal model where the plane-stress contribution is effective over a surface skin depth r_0 and the plane-strain prevails over the remaining central portion. Thus they suggested that:

$$r_0 = \frac{1}{2\pi(1-2\nu)^2}\left(\frac{K_{Ic}}{\sigma_y}\right)^2 \quad (1)$$

where ν is Poisson's ratio and σ_y is the yield stress. Various workers [6] have adopted this approach to describe thickness effects in a wide range of polymers such as polycarbonate, nylon 6.6., polypropylene and poly(butylene terephthalate). However, it should be recognised that there is no theoretical justification for Eq. (1).

The injection moulding process is an exceeding complex phenomenon involving an unsteady flow and heat conduction, and, in the case of semicrystalline thermoplastics, a non-isothermal crystallisation [7]. The result of this crystallisation process is a skin-core structure composed of a surface skin layer with a high orientation and an inner core layer composed of spherulites with a low molecular orientation. It is widely recognised that the mechanical properties of injection moulded semicrystalline thermoplastics are strongly dependent on this morphology of the polymer [7–9]. The built-up of the skin layer strongly depends on molecular weight characteristics and the moulding conditions of the PP [10].

The aim of the present study is to correlate the stress-state, the local morphology and micromechanical properties to the fracture features of virgin and recycled PP. Microhardness has been used to characterise the injection moulding induced morphology. Fracture tests have been carried out by Charpy impact tests, and fracture surfaces were analysed by scanning electron microscopy (SEM).

2. Experimental procedure

2.1. Materials and specimen preparation

For this investigation a commercial isotactic polypropylene (iPP) homopolymer injection grade (SM6100, Montell) was used. To simulate the recycling cycle, iPP was reprocessed following the procedure described in a previous paper [1]. Virgin iPP is refereed as PP-R1. To simulate the recycling steps, PP was processed in a Battenfeld BA 600CDC injection moulding machine, and the moulded specimens obtained were granulated in a knife mill for the next recycling step. This procedure was repeated up to six times and the resultant recycled iPP is refereed as PP-R6. Tensile test specimens and single edge notched bend (SENB) specimens for impact tests were obtained as described in Ref. [1] and [2], respectively.

2.2. Microhardness measurements

Microhardness was measured at room temperature using a Zwick 3213B tester. In a standard Vickers hardness test the indenter is a diamond square-based pyramid with an angle between opposite faces of 136°. The H_v hardness value (MPa) was derived from the residual projected area of indentation according to the expression:

$$H_v = 1.854(F/d^2) \quad (2)$$

where d is the length of the impression diagonal (mm) and F the applied contact load (N).

Microhardness was measured in the centre of each prismatic specimen perpendicular to the injection direction (xy plane), i.e. in the x direction in Fig. 1. Each surface to be tested was ground wet to 1000 emery followed by polishing successively on 3 and 1 μm diamond paste wheels. Hardness readings were taken no nearer than 75 μm from free edges of the sample, and the space between each indent centre was 100 μm. Following the test procedure suggested by Ref. [11], a load of 1 N was applied for 6 s in order to minimise the creep of the sample under the indenter. A minimum of three measurements were made to calculate each microhardness average value.

2.3. Tensile and impact tests

Tensile tests were performed on an Instron 4206 standard testing machine at a crosshead speed of 50 mm/min and at room temperature following ASTM D-638-97. Impact tests were carried out on a CEAST instrumented Charpy pendulum, equipped with a data acquisition unit. SENB specimens were tested under the following conditions: v = 0.57 m/s; mass of the pendulum = 2.182 kg; room temperature; span 50.8 mm. Data acquisition was made with a time interval of 2 μs per point. The impact data were analysed according to the linear elastic fracture mechanics approach (LEFM) [3].

2.4. Fractography

Fracture surfaces of Charpy specimens were studied by SEM in order to determine the micromechanisms of fracture. Direct observation of the fracture surfaces was carried out under low vacuum conditions (20–25 Pa).

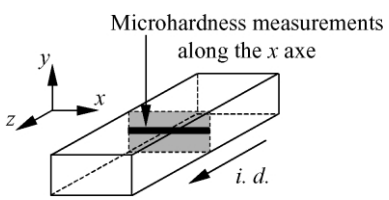

Fig. 1. Schema of microhardness measurements. Indentations were made on the xy plane along the x axe. z is the injection direction (i.d.).

3. Results and discussion

3.1. Microhardness study

The variation of H_v as a function of the distance from the free surface (b) for PP-R1 and PP-R6 is shown in Fig. 2. There can be found common features but also differences between these two curves. The starting H_v values at the skin layer for both materials are similar, and H_v increases with b, reaching the highest values at the core region where H_v is practically constant. However, the differences between PP-R1 and PP-R6 are found at the plateau. PP-R1 reaches the central plateau at lower b values than PP-R6, i.e. closer from the free surface, and the microhardness values are lower for PP-R1 material, which is a consequence of its lower crystallinity [1]. There is no length difference between the two diagonals of the indentations, the fact that H_v has been measured perpendicular to the injection direction explains the isotropy of these results.

It has long been recognised that microhardness provides valuable information about morphological parameters of polymers [12]. Dealing with semicrystalline polymers, the microhardness is proportional to the volume fraction of crystalline material (X_c). Thus, microhardness results imply that X_c is low at the skin layer (small H_v), where the cooling rate is high, and increases towards the interior. Furthermore, H_v is directly correlated to the yield stress of the material [12], and as for X_c, there is an evolution of σ_y across the moulding section, going from low σ_y at the skin layer to higher values at the core region. Although only prismatic specimens have been analysed, it is considered that H_v profile varies similarly in tensile specimens, i.e. from low H_v values at the skin layer to higher ones at the core region.

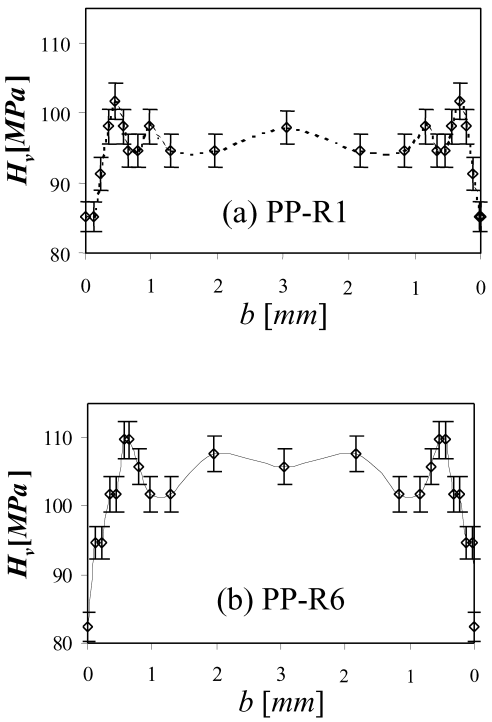

Fig. 2. Microhardness (H_v) profile along the x direction obtained from measurements at the inner xy surface for PP-R1 (a) and PP-R6 (b).

3.2. Failure analysis under tensile loading

During tensile tests different deformation and fracture micromechanisms develop at the skin and core region. Tensile tested PP-R1 and PP-R6 specimens showed a core region where stress-whitened was developed, whereas the skin layer remained transparent (Fig. 3). It has been shown that these whitened regions have craze-like structure [13]. Whitening effect is due to the fact that crazes are highly light reflecting since they have a refractive index which is much lower than that of the bulk polymer [6].

Fig. 4 shows a typical fracture surface of PP-R1 and PP-R6. As can be observed, skin layer breaks at small elongation level, whereas the core region breaks after higher elongation. Supposedly, the skin layer should break at longer elongation than the core region due to the lower crystallinity of the former (see Section 3.1). However, the molecular orientation is so high at the skin layer that it breaks just after yielding and does not show necking [14].

3.3. Fracture analysis under impact loading

All PP-R1 and PP-R6 specimens fractured brittlely, Charpy specimens broke instantaneously after the maximum load was reached and at small deflections. The strain energy density theory [15] postulates that crack propagation is incremental and instability will occur if the increment of the crack growth reaches a critical value. In a purely brittle fracture mode, such as in the case of impact loaded PP, it could be considered that the first crack growth increment immediately reaches the critical value of the material. During the impact test, where the main fracture micromechanism in PP-R1 and PP-R6 is crazing [2], as the external load increases, microscopic crazes are formed together with the development of a local plastic region at the tip of the notch (Fig. 5). This crazed region spreads out with increasing load. When the size of the plastic zone reaches a critical extent and fulfils the unstable condition of deformation, unstable fracture occurs.

Fracture surface morphology of SENB specimens shows

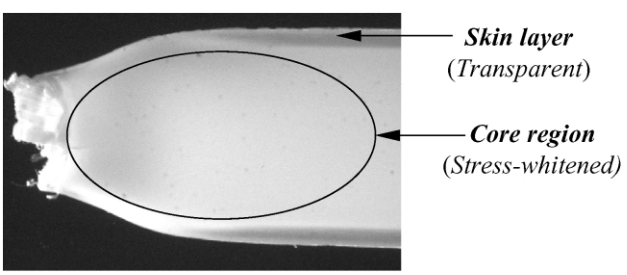

Fig. 3. Tested tensile specimen of PP-R1 showing stress-whitened core and transparent skin layer. PP-R6 exhibits the same features.

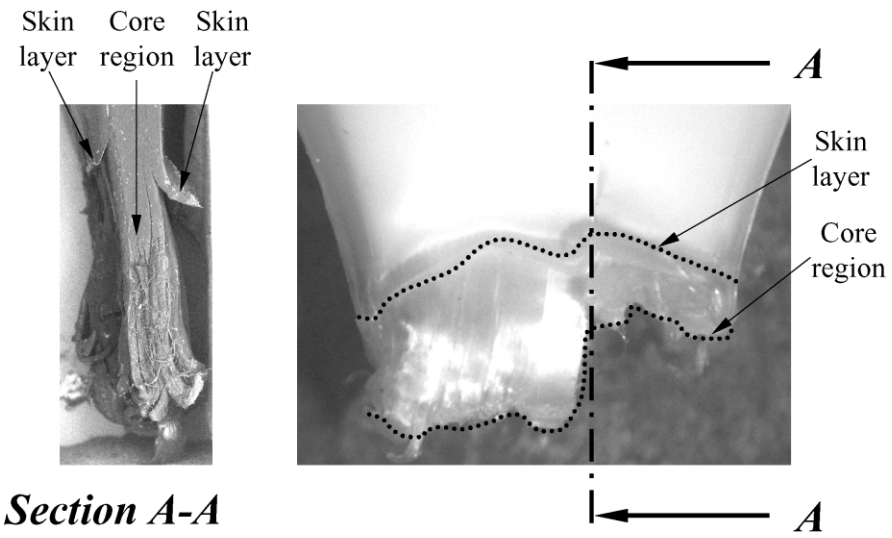

Fig. 4. Typical fracture surface of PP-R1 under tensile loading. PP-R6 exhibits the same features.

several features (Fig. 6). The different crack propagation modes (Fig. 6(a)) generate three distinct morphologies (Fig. 6(b)): (*A*) a fracture induction area where the crack accelerates and the result is a patchwork structure, (*B*) the rough zone where the crack propagates across crazes at different planes, and (*C*) the smooth zone where the crack grows without any plastic deformation. The extension of *A* and *B* zones defines the plastically deformed zone, r_y [16].

3.4. Effects of morphology on fracture micromechanisms

Fig. 7 shows the size of the plastically deformed zone (r_y), measured from the fracture micrographs by optical microscopy, for PP-R1 and PP-R6 as a function of the distance from the free surface (*b*). There are two major features; (a) PP-R1 develops a bigger plastic zone at the notch tip than PP-R6, and (b) in the centre of the specimen the plastically deformed area had propagated further ahead than at the edges of the crack front. The former is explained by the lower degree of crystalline of PP-R1, whereas the latter is related to differences in morphological parameters and stress-state.

Observed r_y is a consequence of the formation of a large number of crazes (Fig. 5). Crazing depends on morphological parameters such as degree of crystallinity (X_c), since the tendency to craze nucleation is enhanced with decreasing X_c [17]. It has been previously pointed out that microhardness, H_v, depends on X_c and that an increase in H_v can be interpreted as a consequence of higher X_c. Thus, and if the effect of X_c is considered separately from other factors, theoretically the size of the zone deformed by crazing should be inversely proportional to H_v. Plastic zone size (r_y) is shown in Fig. 8 as a function of H_v, and as it can be seen, the above hypothetical dependence of r_y on X_c is not fulfilled since r_y increases with H_v. Thus, there should be another factor controlling the crazing mechanism.

3.5. Effects of stress-state on fracture micromechanisms

Crazing is a cavitation process and hence occurs with an increase in volume. Craze initiation therefore usually requires the presence of a dilatational component into the stress tensor and may be enhanced by the presence of triaxial tensile stresses [17]. Thus, the higher the triaxiality is the higher the craze formation ability, and consequently r_y should also be greater.

Table 1 shows the fracture toughness (K_{Ic}) [1] and the surface skin depth (r_0, Eq. (1)) where the plane-stress

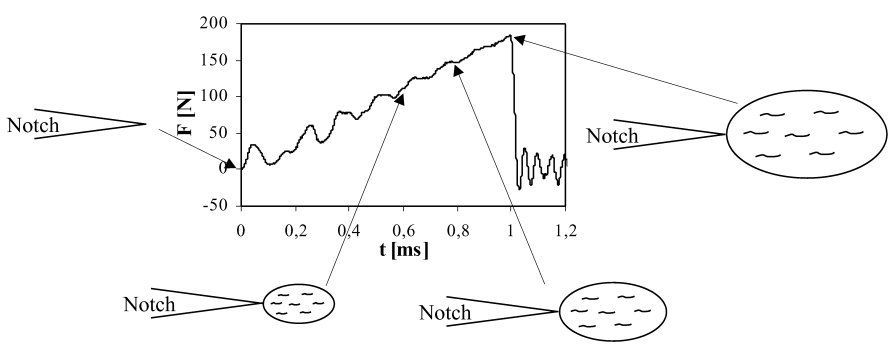

Fig. 5. Development of the plastic zone at the crack tip during the impact test.

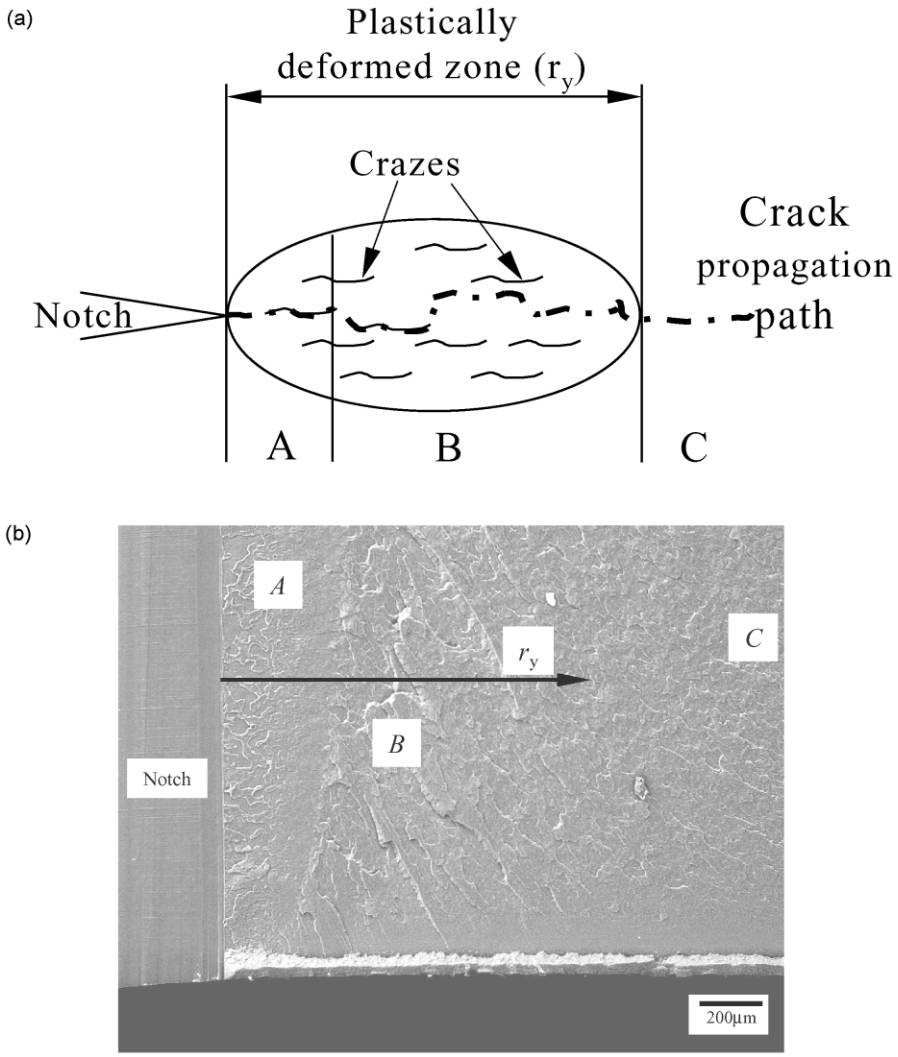

Fig. 6. Schema of the crazed zone at the notch tip (r_y) showing the crack propagation path (a), where *A*, *B* and *C* indicate the fracture induction area, the rough zone and the smooth surface, respectively, and (b) fracture surface micrograph of a Charpy impact test specimen where the arrow delimitates the extension of the crazed zone at a given depth.

contribution is effective for PP-R1 and PP-R6. Based on r_0, three different stress-states have been defined in edge notch specimens. The surfaces ($b = 0$) are in pure plane-stress (biaxial stress-state) while the central region ($b > r_0$) gives rise to plane-strain conditions (triaxial stress-state), and at the transition zone ($0 < b < r_0$) a mixture of plane-strain and plane-stress conditions is assumed.

Fig. 9 shows the three stress-states described above on the r_y vs. b for PP-R1 (Fig. 9(a)) and PP-R6 (Fig. 9(b)). As can be seen, in both cases there is a good correlation between the triaxial stress-state level and the crazed damage zone size (r_y), and it can be postulated that the effect of stress-state on deformation and fracture micromechanisms

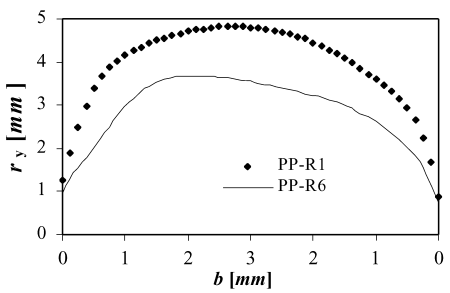

Fig. 7. Plastically deformed zone size (r_y) for PP-R1 (◆) and PP-R6 (—) as a function of the distance from the free surface (b).

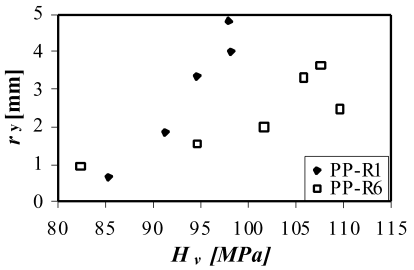

Fig. 8. Plastically deformed zone size (r_y) plotted as a function of microhardness (H_v) for PP-R1 (◆) and PP-R6 (□).

Table 1
Fracture toughness (K_{Ic}) and surface skin depth (r_0, Eq. (1)) where the plane-stress contribution is effective for the virgin (PP-R1) and six times recycled PP (PP-R6)

Sample	K_{Ic} (MPa m$^{1/2}$)[a]	r_0 (mm)[b]
PP-R1	2.23 ± 0.09	2.06
PP-R6	1.96 ± 0.1	1.59

[a] Data taken from Ref. [1].
[b] The calculations have been made with $\nu = 0.3$ and $\sigma_y = 49$ MPa [18].

is higher than that of the morphology (the degree of crystallinity, X_c).

4. Conclusions

The effects of the local morphology, the micromechanical properties and the stress-state on fracture features of virgin and recycled PP have been investigated.

Virgin PP has shown higher microhardness values and bigger plastically deformed zone at the crack tip than recycled one. These two differences are due to the higher crystallinity of the recycled PP.

Otherwise, in both materials, skin layer has shown lower microhardness values and smaller plastic zone extension than the core region. The former phenomenon is suggested to be governed by the different degrees of crystallinity between both regions, whereas the latter is related to the stress-state (triaxial stress-state) rather than to morphological parameters.

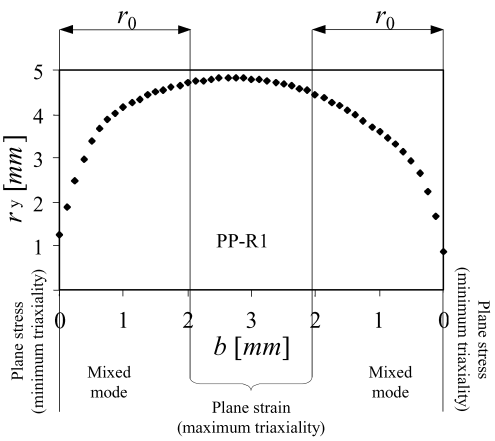

(a)

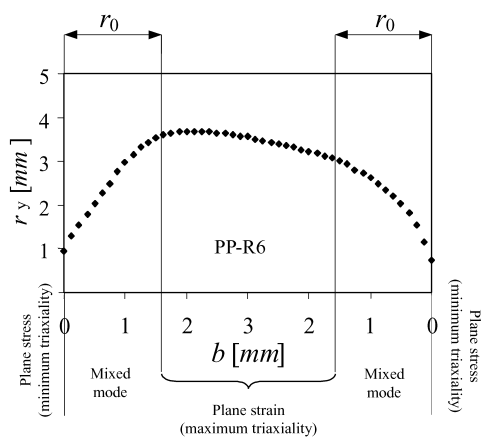

(b)

Fig. 9. Plastically deformed zone size (r_y) and triaxiality as a function of the distance from the free surface (b) for PP-R1 (a), and PP-R6 (b).

Acknowledgements

The authors would like to thank Mr G. Castillo, and Mr L. Aretxabaleta (Department of Mechanics, Mondragon Unibertsitatea) for their helpful discussions.

References

[1] Aurrekoetxea J, Sarrionandia MA, Urrutibeascoa I, Maspoch MLl. J Mater Sci 2001;36:1.
[2] Aurrekoetxea J, Sarrionandia MA, Urrutibeascoa I, Maspoch MLl. J Mater Sci 2001;36:5073.
[3] Williams JG. Fracture mechanics of polymers. Chichester: Ellis Horwood; 1987.
[4] Williams JG, Parvin M. Int J Fract 1975;11:963.
[5] Williams JG, Parvin M. Int J Fract 1975;10:1883.
[6] Kinloch AJ, Young RJ. Fracture behaviour of polymers. London: Applied Science Publishers; 1983.
[7] Fujiyama F. In: Karger-Kocsis J, editor. Polypropylene structure, blends and composites, vol. 1. London: Chapman & Hall; 1995. Chapter 6.
[8] Murphy MW, Thomas K, Bevis MJ. Plast Rubb Process Appl 1988;9:3.
[9] Gahleitner M, Wolfschwenger J, Bachner C, Bernreitner K, Neissl W. J Appl Polym Sci 1996;61:649.
[10] Karger-Kocsis J, Mouzakis DE, Ehrenstein GW, Varga J. J Appl Polym Sci 1999;73:1205.
[11] Flores A, Aurrekoetxea J, Gensler R, Kausch HH, Balta-Calleja FJ. Colloid Polym Sci 1998;276:786.
[12] Balta-Calleja FJ. Trends Polym Sci 1994;2:419.
[13] Liu Y, Kennard CHL, Truss RW, Calos NJ. Polymer 1997;38:2797.
[14] Fujiyama M, Wakino T, Kawasaki Y. J Appl Polym Sci 1998;35:29.
[15] Vu-Khanh T, Fisa B. Theor Appl Fract Mech 1990;13:11.
[16] Gensler R, Plummer CJG, Grein C, Kausch HH. Polymer 2000;41:3809.
[17] Friedrich K. In: Kausch HH, editor. Crazing in polymers. Berlin: Springer-Verlag; 1983. p. 225.
[18] van der Wal A. Ph.D. Thesis, University of Twente; 1996.